

Published in final edited form as:

*J Biomol Screen*. 2014 March ; 19(3): 427–436. doi:10.1177/1087057113499633.

## High-Throughput Fluorescence Anisotropy Screen for Inhibitors of the Oncogenic mRNA-binding Protein, IMP-1

Lily Mahapatra<sup>1</sup>, Chengjian Mao<sup>2</sup>, Neal Andruska<sup>2</sup>, Chen Zhang<sup>3</sup>, and David J. Shapiro<sup>2,\*</sup>

<sup>1</sup>Department of Molecular and Integrative Physiology, University of Illinois, Urbana, IL, USA

<sup>2</sup>Department of Biochemistry, University of Illinois, Urbana, IL, USA

<sup>3</sup>High Throughput Screening Center, School of Chemical Sciences, University of Illinois, Urbana, IL, USA

### Abstract

Cancer cell proliferation is regulated by oncogenes, such as c-Myc. An alternative approach to directly targeting individual oncogenes is to target IMP-1, an oncofetal protein that binds to and stabilizes mRNAs, leading to elevated expression of c-Myc and other oncogenes. Expression of IMP-1 is tightly correlated with a poor prognosis and reduced survival in ovarian, lung and colon cancer. Small molecule inhibitors of IMP-1 have not been reported. We established a fluorescence anisotropy/polarization microplate assay (FAMA) for analyzing binding of IMP-1 to a fluorescein-labeled 93 nucleotide c-Myc mRNA target (flMyc), developed the assay as a highly robust ( $Z'$  factor = 0.60) FAMA-based high throughput screen for inhibitors of binding of IMP-1 to flMyc, and carried out a successful pilot screen of 17,600 small molecules. Our studies support rapidly filtering out toxic non-specific inhibitors using an early cell-based assay in control cells lacking the target protein. The physiologic importance of verified hits from the *in vitro* high throughput screen was demonstrated by identification of the first small molecule IMP-1 inhibitor; a lead compound that selectively inhibits proliferation of IMP-1 positive cancer cells with very little or no effect on proliferation of IMP-1 negative cells.

### Introduction

The oncofetal mRNA binding protein IMP-1/CRD-BP/IGF2BP1 is a multifunctional mRNA binding protein with important roles in mRNA degradation,<sup>1–3</sup> translation,<sup>4</sup> and localization.<sup>5</sup> Overexpression of IMP-1 results in enhanced cell proliferation,<sup>6</sup> suppression of apoptosis,<sup>7</sup> and resistance to taxanes and other anticancer drugs.<sup>8,9</sup> Kaplan-Meier plots show that expression of IMP-1 is tightly correlated with a poor prognosis in ovarian, colon and lung cancer.<sup>10–12</sup> Consistent with an important role in tumor growth and progression, IMP-1 expression is up-regulated by c-Myc<sup>13</sup> and  $\beta$ -catenin,<sup>14</sup> and it is a major regulatory target of *let-7* microRNA.<sup>15</sup> IMP-1, through its capacity to bind to and stabilize mRNAs, increases expression and activity of key oncogenes including c-Myc, K-Ras and ERK (Fig. 1).

\*To whom correspondence should be addressed: djshapir@life.illinois.edu; Fax: 217-244-5858; Phone: 217-333-1788.

IMP-1 binds to a specific sequence that regulates the stability of c-Myc mRNA, stabilizing c-Myc mRNA, increasing levels of c-Myc mRNA and protein and increasing cell proliferation.<sup>12,13</sup> RNAi knockdown of IMP-1 in cell lines from several types of cancers reduces c-Myc levels, inhibits cell proliferation and triggers apoptosis.<sup>12,14</sup> Additionally, IMP-1 binds to MDR1 (multidrug resistance protein 1/P-glycoprotein) mRNA, stabilizing MDR1 mRNA, leading to overexpression of MDR1 and resistance to anticancer drugs.<sup>1,8,9</sup> RNAi knockdown of IMP-1, or expression of *let-7* miRNA, reduces the level of IMP-1, destabilizes and down-regulates MDR1 and increases sensitivity of cancer cells to killing by therapeutically relevant concentrations of taxol, vinblastine and other anticancer drugs.<sup>8,9</sup> Despite its emerging role in both tumor cell proliferation and multidrug resistance, small molecule modulators of IMP-1 have not been reported.

To establish a quantitative real-time assay for binding of IMP-1 to target RNAs that could be developed for high throughput screening (HTS), we developed a fluorescence anisotropy microplate assay (FAMA). Using this assay, test compounds were evaluated for their ability to inhibit binding of IMP-1 to a 93 nucleotide fluorescein-labeled c-Myc mRNA binding site (flMyc).<sup>16</sup> Because the 93 nucleotide c-Myc RNA binding site was too large to synthesize commercially, we developed simple methods for *in vitro* synthesis and fluorescein-labeling of the RNA.

Assays based on fluorescence anisotropy/polarization have emerged as alternatives to earlier assays such as electrophoretic mobility shift assays (EMSA) that can be difficult to adapt for high throughput. These assays are based on changes in fluorescence polarization/anisotropy on binding of a protein to a labeled RNA. When polarized light excites a fluorophore, such as the fluorescein-labeled c-Myc RNA (flMyc), the relatively small flRNA usually undergoes rotational diffusion more rapidly than the time required for light emission (Fig. 2A). Therefore, the position of the flRNA at the time of light emission is largely randomized, resulting in depolarization of most of the emitted light. In contrast, when a protein, such as IMP-1 binds to the flRNA, the larger size and volume of the protein-flRNA complex causes rotation to be slower, increasing the likelihood that the protein-flRNA complex will be in the same plane at the time of light emission as it was at the time of excitation. Therefore, the emitted light remains highly polarized (Fig. 2A). FAMA is ideal for HTS because it is a homogenous, real-time assay that can be used to rapidly assess binding in solution. Fluorescence polarization/anisotropy methods have recently been successfully utilized in HTS to identify small molecule inhibitors of biologically relevant RNA-protein interactions involved in diseases such as influenza and Rift Valley fever virus.<sup>17,18</sup>

In this study, we carried out an unusual purification that selects for biological activity of purified IMP-1, developed the flMyc RNA probe, and performed a pilot screen of 17,600 small molecules from a compound library in the University of Illinois High Throughput Screening Center. From the pilot screen, we identified 33 verified hits that inhibited binding of IMP-1 to flMyc and met fluorescence intensity cutoffs. Since our primary screen was for inhibition of binding of IMP-1 to flMyc, it did not exclude toxic compounds. We retested the hits for specificity by evaluating their ability to inhibit binding of the steroid hormone receptor, progesterone receptor (PR), to its fluorescein-labeled DNA binding site (fl-

progesterone response element; fIPRE). This specificity test was only moderately successful in filtering out compounds that subsequently proved toxic in IMP-1 negative cells. Although previous pilot screens often used orthogonal validation assays such as EMSA and filter binding, these methods may not fully recapitulate the complex milieu of living cells. Therefore, we assessed how effectively and selectively the hits inhibited a key activity of IMP-1; stimulation of cell proliferation. To establish a cell-based assay to filter the hits, we used RNAi knockdown of IMP-1 to confirm that IMP-1 expression was essential for proliferation of IMP-1 positive cells and that IMP-1 RNAi knockdown had no effect on proliferation of IMP-1 negative cells. The cell-based assay identified a substantial number of hits as toxic in the IMP-1 negative cells. This suggests that an early assay in cells that lack the target protein provides a rapid filter to eliminate small molecules exhibiting non-specific binding and toxicity. Our work suggests a screening strategy in which an initial biochemical screen using purified protein identifies hits that target the desired protein-RNA interaction and an early follow-on cell-based assay filters out non-specific and toxic hits. This approach allowed us to identify a lead as the first selective small molecule inhibitor of IMP-1.

## Materials and Methods

Unless otherwise stated, average  $\pm$  SEM is reported for experiments where SEM equals  $\sigma/(\sqrt{n})$ , where  $\sigma$  represents the population standard deviation and  $n$  is the sample size.

### Compound Libraries

The pilot screen chemical library used part of a library of commercially available small molecules from the Chembridge Microformat Library that is maintained in the University of Illinois High Throughput Screening Center. Compounds are stored at  $-20^{\circ}\text{C}$  and arrayed in 384-well plates at concentrations of 1 or 10 mM in DMSO.

### Protein Purification

IMP-1 was purified as described by Nielsen et al.<sup>19</sup> with minor modifications, mostly suggested by Dr. J. Christiansen. Untagged full-length IMP-1 in PET42a (Novagen) was expressed in a strain of BL21DE3pLysS expressing plasmid-encoded tRNAs for rare Arg, Ile and Leu codons (a generous gift of Dr. J. Christiansen). Following protein expression, cells were harvested, broken by sonication in 20 mM Tris-HCl, pH 7.8, 5 mM MgCl<sub>2</sub>, 100 mM KCl, 1 mM DTT and 1.4  $\mu\text{g}/\text{ml}$  aprotinin, Triton X-100 was added to 0.4%, and cell debris was removed by centrifugation at 8,000 RPM at  $4^{\circ}\text{C}$  for 10 minutes. The supernatant was made up to 10% in glycerol, and layered on a sucrose cushion consisting of 1.1 M sucrose, 20 mM Tris-HCl, pH 7.8, 5 mM MgCl<sub>2</sub>, 100 mM KCl, 1 mM DTT and 0.1% Triton X-100 and centrifuged for 2 hours at  $4^{\circ}\text{C}$  at 40,000 RPM. The resulting pellet contains IMP-1 bound to polysomal mRNA. The pellets were washed in 20 mM Tris-HCl, pH 7.8, 5 mM MgCl<sub>2</sub>, 100 mM KCl, 1 mM DTT and 0.1% Triton X-100. IMP-1 was dissociated from polysomal mRNA by resuspending the pellets in 20 mM Tris-HCl, pH 7.8, 5 mM MgCl<sub>2</sub>, 650 mM KCl, 1 mM DTT and 0.1% Triton X-100. The suspension was centrifuged for 1 hour at  $4^{\circ}\text{C}$  at 40,000 RPM. The supernatant was adjusted to 200 mM KCl and 10% glycerol before it was applied to a 2 mL Heparin-Sepharose column (Amersham Biosciences) equilibrated in 20 mM Tris-HCl, pH 7.8, 5 mM MgCl<sub>2</sub>, 200 mM KCl, 1 mM

DTT, 0.1% Triton X-100 and 10% glycerol. After washing with the equilibration buffer, the protein was eluted by the same buffer containing 350 mM KCl. As shown in Figure 2B, the indicated eluted fractions (E, elution) were resolved on a 10% SDS-PAGE gel and visualized by Coomassie blue staining. Purified IMP-1 from fractions E7 and E8 was near homogenous and was used in our studies.

Full-length FLAG-epitope tagged human PR-B (120 kDa) was purified from baculovirus-infected insect cells produced at 5L BioReactor scale in a facility at the University of Colorado Health Sciences Center facility<sup>20</sup> and was a generous gift of Prof. S. Nordeen.

### Synthesis of Fluorescein-labeled c-Myc RNA Probe

The flMyc probe was produced essentially as we describe,<sup>16</sup> with the minor modification of using the MEGAscript kit (Ambion) for *in vitro* transcription.

Standard palindromic cPRE/GRE (5'-f-CTAGATTACAGAAACAATCTGTTCTTAC TCA-3') were synthesized as previously described.<sup>21</sup> Briefly, sense strand oligonucleotide was synthesized with fluorescein (6-FAM) at their 5' ends using phosphoramidite chemistry and PolyPak™ II (Glen Research) purified by the Biotechnology Center (University of Illinois Urbana-Champaign). Oligonucleotide concentrations were calculated from A<sub>260</sub> and the labeled sense strands were annealed with equimolar amounts of unlabeled antisense strands.

### Fluorescence Anisotropy Assays

The fluorescence anisotropy microplate assay (FAMA) buffer was modified from our earlier assay.<sup>16</sup> Anisotropy change represents the difference between the anisotropy measured at each concentration of IMP-1 and the anisotropy value measured in the absence of IMP-1 (flMyc RNA alone). In competition experiments, unlabeled competitors were pre-mixed with the fluorescein-labeled RNA probe before IMP-1 was added. The anisotropy change for IMP-1 binding to flMyc-RNA with no competitor was set to 100%. Percent anisotropy change was calculated as follows: (anisotropy change (plus competitor)/anisotropy change (no competitor))×100.

FAMA for High Throughput Screening was performed in 384-well low volume, flat bottom microplates (Greiner Bio-One). The optimum IMP-1 protein (10 nM) and flMyc RNA (1 nM) concentrations for the assay were chosen because they result in approximately 90% of maximal binding. Assays contained 20 mM Tris-HCl, pH 8.0, 150 mM KCl, 1 mM EDTA, 1 ng/μl tRNA, 1 ng/μl heparin, 0.4 U/μl RNasin, and 500 ng/μl RNase-free BSA. A sequential protocol was used to assess changes in anisotropy, intrinsic fluorescence of test compounds, the compounds' influence on the anisotropy signal of the probe alone, and the ability of compounds to inhibit binding of IMP-1 to flMyc. First, plates were loaded with 10 μl binding buffer containing fluorescein-labeled c-Myc RNA probe (2-fold in binding buffer) with a Matrix PlateMate Plus dispenser (Thermo Scientific) in every well. Then 100 nL of each test compound from the 1 mM compound plates was transferred to each well of the test plates using the Matrix PlateMate Plus robotic pin transfer apparatus. Then fluorescence polarization/anisotropy (FP/FA) was determined using an Analyst HT Plate Reader

(Molecular Devices). FITC FP 480 (excitation) and 535 (emission) filters were used. Then, 10  $\mu$ l of binding buffer and IMP-1 protein (final assay concentration 10 nM) was added to each well except control wells that received 10  $\mu$ l of binding buffer. FP/FA for each well was measured after 15 minutes, when the assay had reached equilibrium as determined from kinetic studies of the ON and OFF rate of IMP-1 binding to flMyc. Thus, in the final assay compounds were tested at 5  $\mu$ M for their ability to inhibit binding of 10 nM of IMP-1 to 1 nM flMyc RNA probe. Columns 23 and 24 on each plate contain DMSO and no test compounds and these wells served as screening controls.

For follow-on tests for specificity, fluorescein-labeled progesterone response element (flPRE) was diluted to 1 nM in a binding buffer containing 15 mM Tris-HCl, pH 7.9, 100 mM KCl, 1 mM dithiothreitol (DTT), 5% glycerol, 0.05% Nonidet<sup>TM</sup> P-40 (NP-40), 100 ng poly dI:dC (non-specific competitor), and 250 ng/ $\mu$ l BSA. The protocol for assessing change in anisotropy was similar to the one described above for the IMP-1:flMyc experiments, except that compounds were tested at a final concentration of 10  $\mu$ M for their ability to inhibit binding of PR to the flPRE DNA probe. The concentration of PR used in the follow-on assay, 35 nM, is not saturating and is highly responsive to inhibition.

### Data Analysis and Hit Scoring

To determine the robustness of our screening assay, the  $Z'$  factor for each plate was calculated as previously described.<sup>22</sup> A  $Z'$  factor greater than 0.5 describes a robust assay suitable for high throughput screening.<sup>22</sup> The results from the pilot screen were further analyzed using a simple program we developed to evaluate and score different parameters and identify the most promising compounds from the HTS. Initially, compounds that altered the overall fluorescence intensity by  $\geq 30\%$  compared to control wells were considered as either enhancers or quenchers and were excluded from further analysis. The remaining compounds were evaluated for percent inhibition which was calculated relative to the assay plate control wells, where % inhibition =  $(1 - ((mA_{Comp} - mA_{Min}) / (mA_{Max} - mA_{Min}))) \times 100$ , where the assay minimum ( $mA_{Min}$ ) is flMyc RNA alone and the assay maximum ( $mA_{Max}$ ) is flMyc with IMP-1 protein. Although there is no universally accepted standard of what change in signal constitutes a “hit” suitable for further evaluation, some researchers consider that any small molecule that results in a change of more than three standard deviations from the mean is appropriate for further study. The average change in anisotropy for the compounds in the pilot HTS was  $86.7 \text{ mA} \pm 6.7$  (average  $\pm$  S.D.). The S.D. is 7.7% ( $6.7/86.7$ ), and  $3 \times$  S.D. is  $\sim 25\%$ . We therefore carried out further analysis of small molecules that, when present at 5  $\mu$ M, altered the average change in anisotropy for binding of IMP-1 to flMyc by at least 25%. Compounds that met fluorescence intensity criteria and the percent inhibition cutoff were considered to be primary hits and were cherry-picked for follow-on assays.

### Cell Culture and siRNA Transfection

IMP-1 positive IGROV-1 ovarian cancer cells and IMP-1 negative PC-3 prostate cancer cells were used in cell-based experiments. IGROV-1 cells were maintained in phenol-red free RPMI 1640 with 10% fetal bovine serum (FBS) and PC-3 cells were maintained in DMEM-F12 with 10% FBS. Cells were grown in monolayer and were maintained at 37 $^{\circ}$  C

with 5% CO<sub>2</sub>. IGROV-1 and PC-3 cells were plated in 96-well plates at a density of 1,000 cells/well and transfected with an IMP-1 siRNA SMARTpool (Dharmacon) or a non-coding control siRNA using Dharmafect 1 transfection reagent (Dharmacon) according to the supplier's protocol. 5 days after transfection cell viability was determined using CellTiter 96 Aqueous One Solution Reagent (Promega). For both cell lines relative cell proliferation was calculated as previously described.<sup>23</sup>

### Testing Hits for Inhibition of Cell Proliferation

IGROV-1 and PC-3 cells were maintained and plated in 96-well plates as described above. Each cell line was plated in growth medium 24 hours before treatment. Treatment medium containing either 0.4% DMSO (vehicle) or inhibitor compounds at a final concentration of 20  $\mu$ M in DMSO. After 3 days, cell viability was determined using Promega CellTiter 96 Aqueous One Solution Reagent (MTS). For each compound percent inhibition of cell proliferation was calculated relative to assay plate DMSO controls, which were set to 0% inhibition. Small molecules were considered potential leads if percent inhibition of proliferation of the IMP-1 positive IGROV-1 cells was at least 3 fold higher than percent inhibition of the control IMP-1 negative PC-3 cells.

### Western Blots

Cells were trypsinized, resuspended in their respective culture media, and plated into 6-well plates at a density of 300,000 cells/well. Cells were harvested, washed in ice-cold phosphate-buffered saline (PBS), and whole-cell extracts were prepared in lysis buffer containing 1 $\times$  radioimmunoprecipitation assay (RIPA) buffer (Millipore), 1 mM EGTA, 30 mM NaF, 2.5 mM sodium pyrophosphate, 1 mM sodium orthovanadate, 1 mM  $\beta$ -glycerol phosphate, 1 mM phenylmethylsulfonyl fluoride, and 1 tablet of protease inhibitor cocktail (Roche). Cells were collected, and debris was pelleted by centrifugation at 15,000 *g* for 10 minutes at 4°C. The supernatants were collected and stored at -20°C. Then, 20  $\mu$ g total protein was loaded onto 10% (v/v) sodium dodecyl sulfate polyacrylamide gel electrophoresis (SDS-PAGE) gels, separated, and transferred to nitrocellulose (GE Healthcare). IMP-1 protein was detected using IMP-1 antibody sc-21026 (Santa Cruz) and  $\beta$ -actin internal standard was detected using antibody A1978 (Sigma).

## Results

### Validation of the High Throughput Screening Assay

We developed the fluorescence anisotropy microplate assay (FAMA) for analyzing the interaction of RNA and DNA binding proteins with their recognition sequences.<sup>16,21</sup> In demonstrating the utility of FAMA for analysis of RNA-protein interactions, we examined the ability of CRD-BP/IMP-1 expressed in *E. coli* and renatured from inclusion bodies to bind to a fluorescein-labeled c-Myc (fMyc) RNA binding site. Binding was low-affinity with an apparent  $K_D$  of several hundred nM.<sup>16</sup> Christiansen, Nielsen and coworkers reported that epitope tagged IMP-1 binds poorly to RNAs<sup>24</sup> and developed an expression system for recombinant untagged IMP-1 using *E. coli* stably expressing several rare tRNAs and a purification protocol that selects for biologically active IMP-1.<sup>19</sup> We expressed and purified

IMP-1 using an update of this expression-purification system and obtained purified untagged IMP-1 that was >90% homogeneous (Fig. 2B).

To identify small molecule inhibitors that target IMP-1, we used modified binding conditions and a far more active IMP-1 preparation to update and improve our earlier assay for IMP-1 binding to flMyc.<sup>16</sup> Purified untagged recombinant IMP-1 exhibited saturable high-affinity binding to the fluorescein-labeled 93 nucleotide (nt) c-Myc RNA site (starting at nt 1705), which contains the IMP-1 binding site (Fig. 2C). Under these binding conditions, the apparent  $K_d$  (the protein concentration at which 50% of the probe was bound) for IMP-1 binding to the flMyc was ~3 nM. Based on the binding data (Fig. 2C), we selected 10 nM IMP-1 for screening. 10 nM IMP-1 yields approximately 90% of maximum binding to flMyc, resulting in a large anisotropy change ( $\Delta$  mA) and a robust assay, while remaining highly responsive to inhibition by small molecules. In this assay, small molecule inhibitors will reduce the anisotropy change seen on binding of IMP-1 to flMyc (Fig. 2A).

Binding of IMP-1 to the flMyc RNA is sequence and structure specific. Because IMP-1 binds unstructured single-stranded RNA, we tested the possibility that IMP-1 primarily interacts with the charged phosphate backbone. With the identification of an important role for polyphosphate in blood clotting,<sup>25</sup> polyphosphate with a length similar to the flMyc RNA became available to us for testing. Even at 1,000 fold molar excess, polyphosphate does not compete for IMP-1 binding (Fig. 2D). Therefore, interaction with the charged phosphate backbone is not responsible for high-affinity binding of IMP-1 to RNAs. Binding of IMP-1 to flMyc was specific, as tRNA, even at 1,000 fold molar excess, had minimal ability to compete for binding (Fig. 2D). Addition of the unlabeled c-Myc RNA resulted in a concentration-dependent reduction in binding. A 2.5 fold molar excess of the unlabeled c-Myc RNA reduced binding of IMP-1 to flMyc by approximately 50% (Fig. 2D).

The performance of the optimized binding assay was evaluated for its stability. Under our assay conditions, binding of IMP-1 to flMyc is highly stable at room temperature and insensitive to changes in DMSO concentration. Using 10 nM IMP-1 and screening conditions, after 60 minutes at 25°C, activity was 97% of the initial activity ( $\Delta$  mA at 60 min was  $91.1 \pm 1.3$  vs. initial  $\Delta$  mA of  $94.1 \pm 0.3$ ; Fig. 2E). DMSO at the concentration to be used in the screen, and at twice that concentration, had no effect on binding of IMP-1 to flMyc (Fig. 2F). Thus, our assay had the requisite qualities for evaluation in a medium-scale pilot screen.

### Pilot Screen for IMP-1 Inhibitors

To validate the assay and to identify small molecules that inhibit binding of IMP-1 protein to flMyc RNA, we carried out a pilot screen using 17,600 compounds (Plates 1–50) from the Chembridge Microformat Library. The performance of the optimized binding assay for use in HTS was evaluated for robustness by calculating the  $Z'$  factor for each of the 50 plates screened. The assay demonstrates robust performance with a mean  $Z'$  factor of  $0.60 \pm 0.06$  (average  $\pm$  S.D.) (Fig. 3A) and a signal to noise (S/N) of 12.4. The average change in anisotropy for the compounds in the pilot screen was  $86.7 \text{ mA} \pm 6.7$  (average  $\pm$  S.D.). The pilot screen statistical parameters are summarized in Table 1.

For the primary screen, compounds exhibiting increases or decreases  $\geq 30\%$  in total fluorescence intensity compared to controls were considered as either enhancers or quenchers and were excluded from analysis. Similar cutoffs have been used on other FP/FA screens.<sup>26,27</sup> For the remaining compounds, we chose a cutoff of at least 25% inhibition (which is  $\sim 3\times$  S.D.) at a final compound concentration of 5  $\mu\text{M}$  and identified 57 primary hits (hit rate 0.32%, 57/17600). Figure 3B is a scatterplot for the 17,600 compounds from the pilot screen.

To validate the 57 hits, we compared their ability to inhibit a control protein-nucleic acid interaction, binding of progesterone (PR), a steroid hormone receptor, to its DNA binding site, the fluorescein-labeled progesterone response element (fIPRE) (Fig 4A) to their ability to inhibit IMP-1 binding to fIMyc. Triplicate assays in small volume 384-well plates used the same method described for the primary screen. At 5  $\mu\text{M}$ , 33 compounds inhibited binding of IMP-1 to fIMyc by  $>25\%$  (Fig 4B). Our counterscreen for specificity used binding of PR to the fIPRE in part because it exhibits a change in anisotropy whose magnitude is similar to that seen for the primary assay using IMP-1 and fIMyc (Fig. 4A). Our aim was to quickly identify potential false positives that displayed high-affinity for non-specific nucleic acid sequence or binding proteins rather than for the IMP-1:cMyc interaction and to identify small molecules that display a high-affinity for DNA, such as ethidium bromide and other DNA intercalators. To provide a stringent test for specificity, we evaluated the ability of the verified hits to inhibit binding of PR to the fIPRE at 10  $\mu\text{M}$ , twice the concentration used in the IMP-1 screen and verification assays. As shown in Figure 4B, only 3 of the 33 verified hits exhibited greater than 25% inhibition of PR:fIPRE binding.

### Evaluating Hits for Inhibition of Cell Proliferation

Elevated expression of IMP-1 in cancer cells is associated with increased cell proliferation, which likely stems from stabilizing c-Myc and other oncogene mRNAs (Fig. 1). Evaluating the ability of verified hits that inhibit binding of IMP-1 to c-Myc to also inhibit effects of IMP-1 on cell proliferation provides a critical test of their effect on a key cancer-related function of IMP-1. To establish the cell proliferation assay, we carried out RNAi knockdown of IMP-1 in IMP-1 positive IGROV-1 ovarian cancer and in IMP-1 negative PC-3 prostate cancer cells (Supplementary Figure 1) in 96-well plates using a control non-coding (NC) siRNA and IMP-1 siRNA. After 5 days, MTS assays were performed and relative percent inhibition of cell proliferation was determined for each cell line.<sup>23</sup> Compared to IGROV-1 cells transfected with the control siRNA, RNAi knockdown of IMP-1 caused an 80% decrease in IGROV-1 cell proliferation. In contrast, compared to transfection with the control siRNA, transfection of the IMP-1 negative PC-3 cells with IMP-1 siRNA had no effect on cell proliferation (Supplementary Figure 1).

We evaluated the effects of all the verified inhibitors from the *in vitro* pilot screen in cell proliferation assays in IMP-1 positive IGROV-1 cells and IMP-1 negative PC-3 cells. Our recent study identifying a small molecule inhibitor of androgen receptor confirms that PC-3 cells are a suitable toxicity control and are quite sensitive to small molecules exhibiting non-specific toxicity.<sup>28</sup> Data is shown for a lead inhibitor and for representatives of the other



classes of small molecules (Fig. 5). The lead small molecule inhibits proliferation of IMP-1 positive IGROV-1 cells, with very little or no effect on IMP-1 negative PC-3 cells (Fig. 5). Our lead small molecule inhibited binding of IMP-1 to flMyc ( $72 \pm 3.6\%$  inhibition at  $5 \mu\text{M}$ ) and does not inhibit binding of PR to the flPRE ( $-31 \pm 3.2\%$  inhibition at  $10 \mu\text{M}$ ). Thus, the lead compound demonstrated efficacy and selectivity both in *in vitro* assays using purified proteins and in cell-based assays. Additional evidence of the robust nature of our screen is shown by the fact that the lead inhibitor had a Z-score of  $-6.8$  and was clearly differentiated from the other compounds on its HTS plate (Supplementary Figure 2).

## Discussion

Expression of IMP-1 is implicated in several human cancers. While Kaplan-Meier survival plots show a tight correlation between IMP-1 expression and survival ( $p < 0.05$  for ovarian, lung and colon cancer), IMP-1 is also strongly implicated in melanomas<sup>6,8,29</sup> and other cancers. IMP-1 is an oncofetal protein expressed in fetal cells and cancer cells and nearly absent in most somatic cells.<sup>30,31</sup> Thus, IMP-1 is an excellent therapeutic target. Although a high-affinity binding site for IMP-1 that is implicated in regulation of c-Myc mRNA degradation was identified a number of years ago, small molecule biomodulators to probe the actions of IMP-1 and inhibit its activity in cancer cells have not been described. The substantial  $>90$  nucleotide size of the high-affinity IMP-1 binding site in c-Myc mRNA, the lack of a clear consensus IMP-1 RNA binding site,<sup>32,33</sup> and wide variations in the affinity of observed IMP-1 preparations for RNA<sup>1,16,19</sup> all complicate development of a high throughput screen. We show that purified IMP-1 binds with high-affinity and specificity to the c-Myc binding site. Even at a 1,000 fold molar excess, tRNA and polyphosphate had very little ability to compete with flMyc for IMP-1 binding (Fig. 2D). Thus, binding of IMP-1 to flMyc exhibited the requisite specificity for HTS.

Our primary screen used an *in vitro* assay for inhibition of binding of purified IMP-1 to flMyc rather than an assay for inhibition of cell proliferation for several reasons. In our hands, it is difficult to obtain the requisite reproducibility in cell-based assays for proliferation inhibitors in 384-well plates. More important, the *in vitro* assay using purified IMP-1 provides direct evidence that the primary hits actually inhibit the desired target—the IMP-1:flMyc interaction. Although recent studies show that IMP-1 stabilizes numerous mRNAs,<sup>32</sup> we focused on identifying small molecule inhibitors of IMP-1 binding to c-Myc mRNA because the specific sequence on c-Myc mRNA, the coding region determinant (starting at nt 1705), is the best defined and most extensively studied IMP-1 binding site. For other oncogene mRNAs stabilized by IMP-1, the IMP-1 binding sites are poorly defined.<sup>1,3</sup> We performed a pilot screen of 17,600 small molecules and identified 30 compounds that showed selective inhibition of IMP-1 binding to flMyc RNA and did not inhibit binding by the control DNA binding protein, PR to its DNA binding site, the PRE. We further evaluated the candidate compounds in physiologically relevant assays that are important to IMP-1's function by assessing cell proliferation in IMP-1 positive and negative control cells. By complementing *in vitro* assays to analyze specific inhibition of IMP-1:c-Myc binding with cell-based assays that evaluate an important biological endpoint in cancer cells, we identified a lead small molecule inhibitor of IMP-1.

Identifying inhibitors of RNA binding proteins is challenging.<sup>34,35</sup> Interestingly, we found that most of the compounds identified from our *in vitro* studies did not fail to work in intact cells; rather, they were toxic in a control cell line. This suggests that future high throughput screening campaigns to identify inhibitors of RNA-binding proteins may benefit from initial use of biochemical assays to identify specific inhibitors with early follow-on cell-based filtering assays to evaluate toxicity. This approach not only identifies specific inhibitors using *in vitro* binding, but characterizes a subset of those compounds exhibiting an important physiological function.

This work represents a promising start towards identification of small molecule inhibitors of IMP-1 and describes a path for HTS to identify additional small molecule IMP-1 biomodulators. The lead inhibitor we describe represents an important initial biomodulator for laboratory studies and further characterization; it is a candidate for structure-activity relationship studies and medicinal chemistry optimization to evaluate its ultimate therapeutic potential.

## Supplementary Material

Refer to Web version on PubMed Central for supplementary material.

## Acknowledgments

We are most grateful to Dr. J. Christiansen for the IMP-1 expression plasmid, the modified *E. coli* strain for expressing IMP-1 and for information on IMP-1 purification and to Dr. S. Nordeen for the purified PR.

### Support

Supported by institutional funds and in part by NIH DK-017909 and NIH R21CA173527.

## References

1. Sparanese D, Lee CH. CRD-BP shields c-myc and MDR-1 RNA from endonucleolytic attack by a mammalian endoribonuclease. *Nucleic Acids Res.* 2007; 35:1209–1221. [PubMed: 17264115]
2. Brewer G, Ross J. Regulation of c-myc mRNA stability in vitro by a labile destabilizer with an essential nucleic acid component. *Mol. Cell Biol.* 1989; 9:1996–2006. [PubMed: 2747642]
3. Elcheva I, Goswami S, Noubissi FK, et al. CRD-BP protects the coding region of betaTrCP1 mRNA from miR-183-mediated degradation. *Mol. Cell.* 2009; 35:240–246. [PubMed: 19647520]
4. Weinlich S, Huttelmaier S, Schierhorn A, et al. IGF2BP1 enhances HCV IRES-mediated translation initiation via the 3'UTR. *RNA.* 2009; 15:1528–1542. [PubMed: 19541769]
5. Patel VL, Mitra S, Harris R, et al. Spatial arrangement of an RNA zipcode identifies mRNAs under post-transcriptional control. *Genes Dev.* 2012; 26:43–53. [PubMed: 22215810]
6. Elcheva I, Tarapore RS, Bhatia N, et al. Overexpression of mRNA-binding protein CRD-BP in malignant melanomas. *Oncogene.* 2008; 27:5069–5074. [PubMed: 18454174]
7. Mongroo PS, Noubissi FK, Cuatrecasas M, et al. IMP-1 displays cross-talk with K-Ras and modulates colon cancer cell survival through the novel proapoptotic protein CYFIP2. *Cancer Res.* 2011; 71:2172–2182. [PubMed: 21252116]
8. Craig EA, Spiegelman VS. Inhibition of coding region determinant binding protein sensitizes melanoma cells to chemotherapeutic agents. *Pigment Cell Melanoma Res.* 2012; 25:83–87. [PubMed: 21981993]
9. Boyerinas B, Park SM, Murmann AE, et al. Let-7 modulates acquired resistance of ovarian cancer to Taxanes via IMP-1-mediated stabilization of multidrug resistance 1. *Int. J. Cancer.* 2012; 130:1787–1797. [PubMed: 21618519]

10. Gu L, Shigemasa K, Ohama K. Increased expression of IGF II mRNA-binding protein 1 mRNA is associated with an advanced clinical stage and poor prognosis in patients with ovarian cancer. *Int. J. Oncol.* 2004; 24:671–678. [PubMed: 14767552]
11. Dimitriadis E, Trangas T, Milatos S, et al. Expression of oncofetal RNA-binding protein CRD-BP/IMP1 predicts clinical outcome in colon cancer. *Int. J. Cancer.* 2007; 121:486–494. [PubMed: 17415713]
12. Kobel M, Weidensdorfer D, Reinke C, et al. Expression of the RNA-binding protein IMP1 correlates with poor prognosis in ovarian carcinoma. *Oncogene.* 2007; 26:7584–7589. [PubMed: 17546046]
13. Noubissi FK, Nikiforov MA, Colburn N, et al. Transcriptional Regulation of CRD-BP by c-myc: Implications for c-myc Functions. *Genes Cancer.* 2010; 1:1074–1082. [PubMed: 21779431]
14. Noubissi FK, Elcheva I, Bhatia N, et al. CRD-BP mediates stabilization of betaTrCP1 and c-myc mRNA in response to beta-catenin signalling. *Nature.* 2006; 441:898–901. [PubMed: 16778892]
15. Boyerinas B, Park SM, Shomron N, et al. Identification of let-7-regulated oncofetal genes. *Cancer Res.* 2008; 68:2587–2591. [PubMed: 18413726]
16. Mao C, Flavin KG, Wang S, et al. Analysis of RNA-protein interactions by a microplate-based fluorescence anisotropy assay. *Anal. Biochem.* 2006; 350:222–232. [PubMed: 16448619]
17. Ellenbecker M, Lanchy JM, Lodmell JS. Identification of Rift Valley fever virus nucleocapsid protein-RNA binding inhibitors using a high-throughput screening assay. *J. Biomol. Screen.* 2012; 17:1062–1070. [PubMed: 22644268]
18. Cho EJ, Xia S, Ma LC, et al. Identification of influenza virus inhibitors targeting NS1A utilizing fluorescence polarization-based high-throughput assay. *J. Biomol. Screen.* 2012; 17:448–459. [PubMed: 22223052]
19. Nielsen J, Kristensen MA, Willemoes M, et al. Sequential dimerization of human zipcode-binding protein IMP1 on RNA: a cooperative mechanism providing RNP stability. *Nucleic Acids Res.* 2004; 32:4368–4376. [PubMed: 15314207]
20. Melvin VS, Edwards DP. Expression and purification of recombinant human progesterone receptor in baculovirus and bacterial systems. *Methods Mol. Biol.* 2001; 176:39–54. [PubMed: 11554337]
21. Wang SY, Ahn BS, Harris R, et al. Fluorescence anisotropy microplate assay for analysis of steroid receptor-DNA interactions. *BioTechniques.* 2004; 37:810–817.
22. Zhang JH, Chung TD, Oldenburg KRA. Simple Statistical Parameter for Use in Evaluation and Validation of High Throughput Screening Assays. *J. Biomol. Screen.* 1999; 4:67–73. [PubMed: 10838414]
23. Andruska N, Mao C, Cherian M, et al. Evaluation of a luciferase-based reporter assay as a screen for inhibitors of estrogen-ERalpha-induced proliferation of breast cancer cells. *J. Biomol. Screen.* 2012; 17:921–932. [PubMed: 22498909]
24. Nielsen J, Christiansen J, Lykke-Andersen J, et al. A family of insulin-like growth factor II mRNA-binding proteins represses translation in late development. *Mol. Cell Biol.* 1999; 19:1262–1270. [PubMed: 9891060]
25. Muller F, Mutch NJ, Schenk WA, et al. Platelet polyphosphates are proinflammatory and procoagulant mediators in vivo. *Cell.* 2009; 139:1143–1156. [PubMed: 20005807]
26. Mao C, Patterson NM, Cherian MT, et al. A new small molecule inhibitor of estrogen receptor alpha binding to estrogen response elements blocks estrogen-dependent growth of cancer cells. *J. Biol. Chem.* 2008; 283:12819–12830. [PubMed: 18337247]
27. Nakayama GR, Bingham P, Tan D, et al. A fluorescence polarization assay for screening inhibitors against the ribonuclease H activity of HIV-1 reverse transcriptase. *Anal. Biochem.* 2006; 351:260–265. [PubMed: 16527235]
28. Cherian MT, Wilson EM, Shapiro DJ. A competitive inhibitor that reduces recruitment of androgen receptor to androgen-responsive genes. *J. Biol. Chem.* 2012; 287:23368–23380. [PubMed: 22589544]
29. Craig EA, Weber JD, Spiegelman VS. Involvement of the mRNA binding protein CRD-BP in the regulation of metastatic melanoma cell proliferation and invasion by hypoxia. *J. Cell Sci.* 2012; 125:5950–5954. [PubMed: 23038779]

30. Ioannidis P, Mahaira L, Papadopoulou A, et al. CRD-BP: a c-Myc mRNA stabilizing protein with an oncofetal pattern of expression. *Anticancer Res.* 2003; 23:2179–2183. [PubMed: 12894594]
31. Hansen TV, Hammer NA, Nielsen J, et al. Dwarfism and impaired gut development in insulin-like growth factor II mRNA-binding protein 1-deficient mice. *Mol. Cell Biol.* 2004; 24:4448–4464. [PubMed: 15121863]
32. Hafner M, Landthaler M, Burger L, et al. Transcriptome-wide identification of RNA-binding protein and microRNA target sites by PAR-CLIP. *Cell.* 2010; 141:129–141. [PubMed: 20371350]
33. Bell JL, Wachter K, Muhleck B, et al. Insulin-like growth factor 2 mRNA-binding proteins (IGF2BPs): post-transcriptional drivers of cancer progression? *Cell Mol. Life Sci.* 2012; 69:1–19. [PubMed: 22009453]
34. Thomas JR, Hergenrother PJ. Targeting RNA with small molecules. *Chem. Rev.* 2008; 108:1171–1224. [PubMed: 18361529]
35. DeJong ES, Luy B, Marino JP. RNA and RNA-protein complexes as targets for therapeutic intervention. *Cur. Top. Med. Chem.* 2002; 2:289–302.

# IMP-1/CRD-BP Action in Cancer

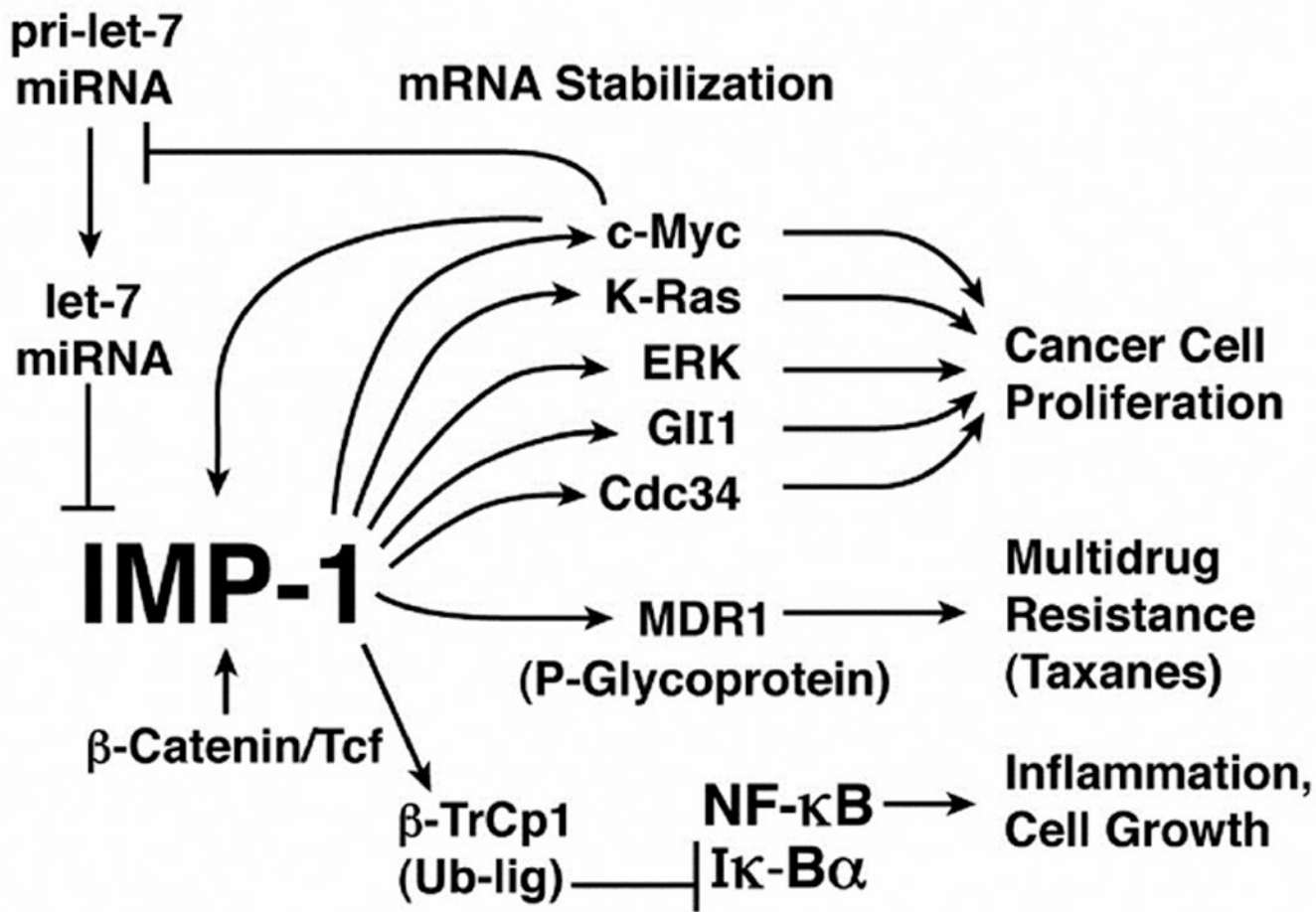


**Figure 1.** Schematic representation of IMP-1 action in stabilizing mRNAs important in cancer.

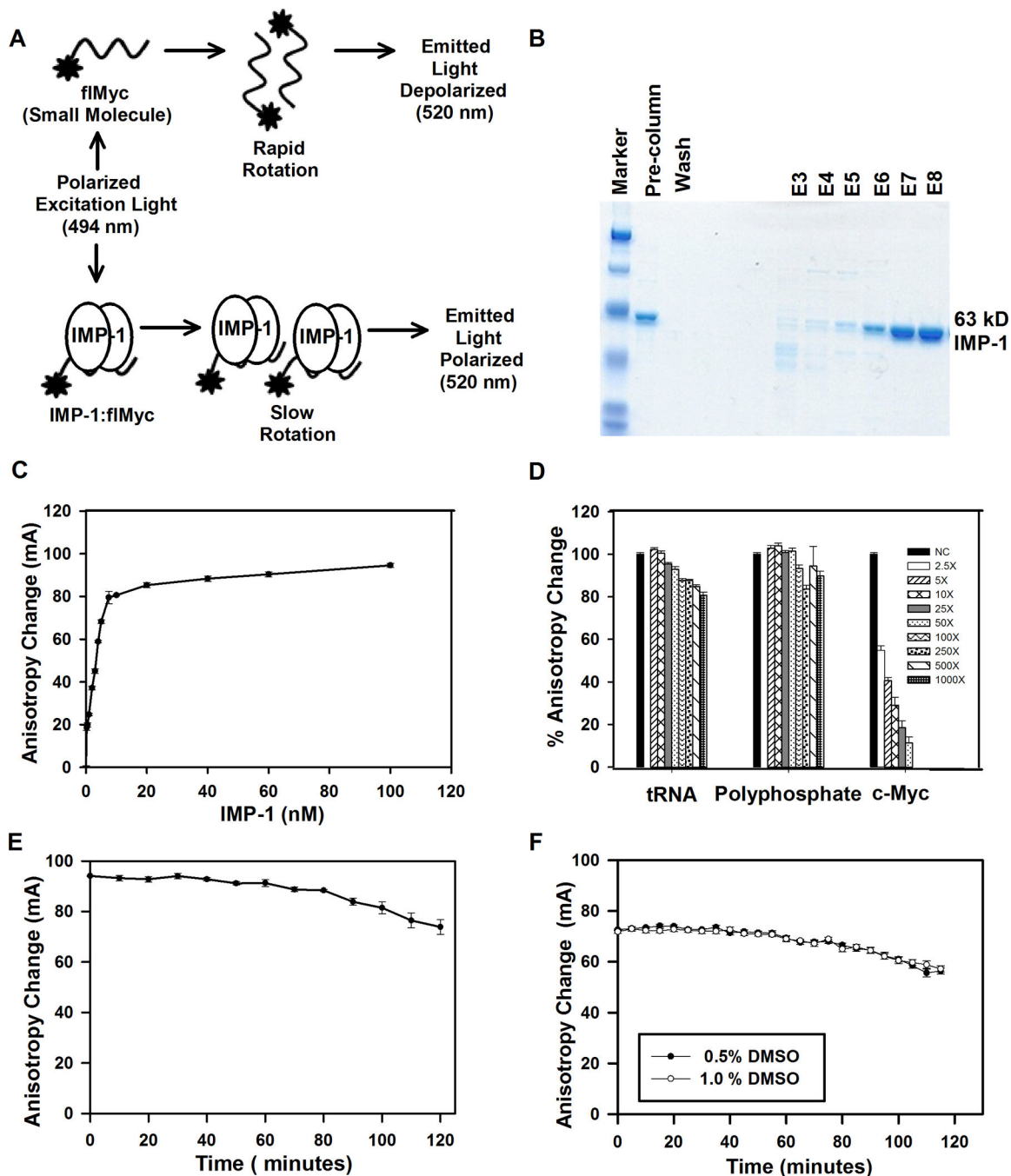


**Figure 2.** Development of fluorescence anisotropy microplate assay (FAMA) for high throughput screening to identify inhibitors of IMP-1 binding to fIMyc. (A) Schematic representation of FAMA to evaluate binding of IMP-1 protein to fIMyc RNA probe. (B) Purification of IMP-1. (C and D) Binding of IMP-1 to fIMyc is saturable and specific. (C) Dose-response study of binding of IMP-1 to fIMyc RNA. Increasing amounts of IMP-1 were incubated with 1 nM fIMyc RNA probe. (D) Competition experiments to assess the specificity of IMP-1 binding to fIMyc RNA. 10 nM IMP-1 protein was added to reactions containing 1 nM fIMyc

RNA, and the indicated molar excess of unlabeled specific c-Myc mRNA fragment, or the non-specific competitors, tRNA, or polyphosphate. The anisotropy change for IMP-1 binding to flMyc RNA with no competitor was set to 100%. **(E and F)** Stability of the IMP-1:flMyc complex at room temperature and at different DMSO concentrations. **(E)** Binding of IMP-1 to flMyc RNA is stable for 1 hour at room temperature. Measurements were made of the same wells over 120 minutes. **(F)** DMSO at the concentration to be used in the screen (0.5%), and at twice that concentration (1%), had negligible effect on binding of IMP-1 to flMyc. The data in panels C, D, E and F represents the average  $\pm$  SEM (n=4).

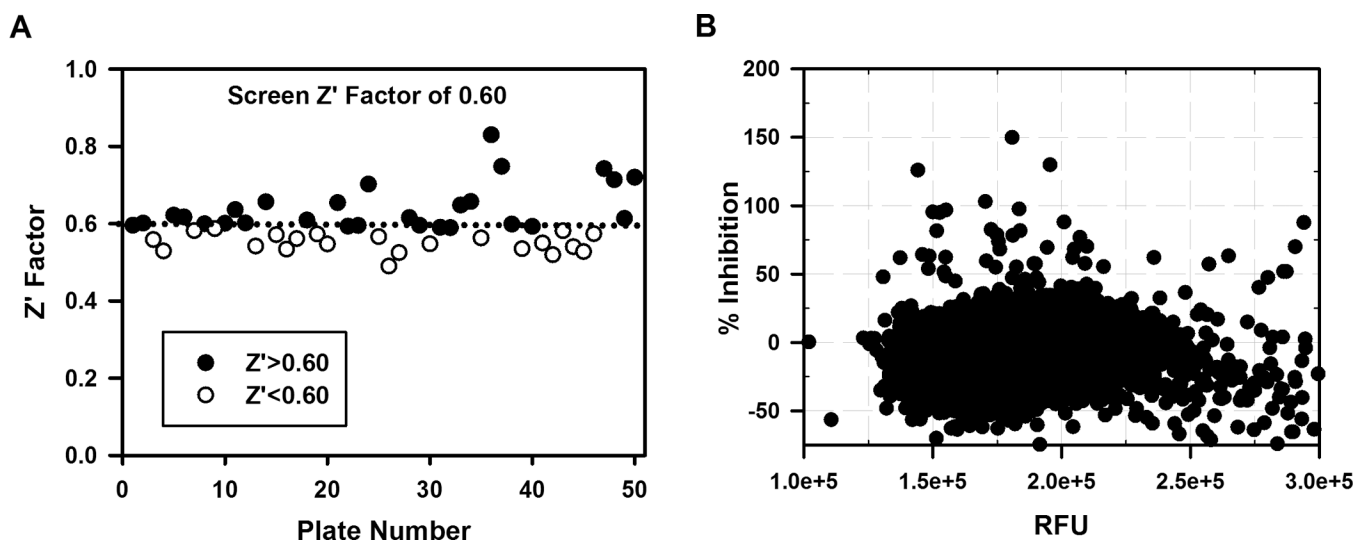


**Figure 3.**

Assay validation and high throughput screening results. **(A)** Assessment of screen robustness for the 50 plates screened using the  $Z'$  factor. The dotted line demarcates a  $Z'$  factor of 0.6, the average  $Z'$  factor for the 50 plate pilot screen. **(B)** Scatterplot of 17,600 small molecules screened from 50 plates in pilot HTS. A percent inhibition  $>100\%$  means the small molecule reduced the anisotropy to a level lower than was seen with fIMyc alone. RFU (relative fluorescence unit) represents the sum of the fluorescence intensities in the parallel and perpendicular channel for a given compound and  $\% \text{ inhibition} = (1 - ((mA_{\text{Comp}} - mA_{\text{Min}}) / (mA_{\text{Max}} - mA_{\text{Min}}))) \times 100$ . Data from HTS are single point assays.



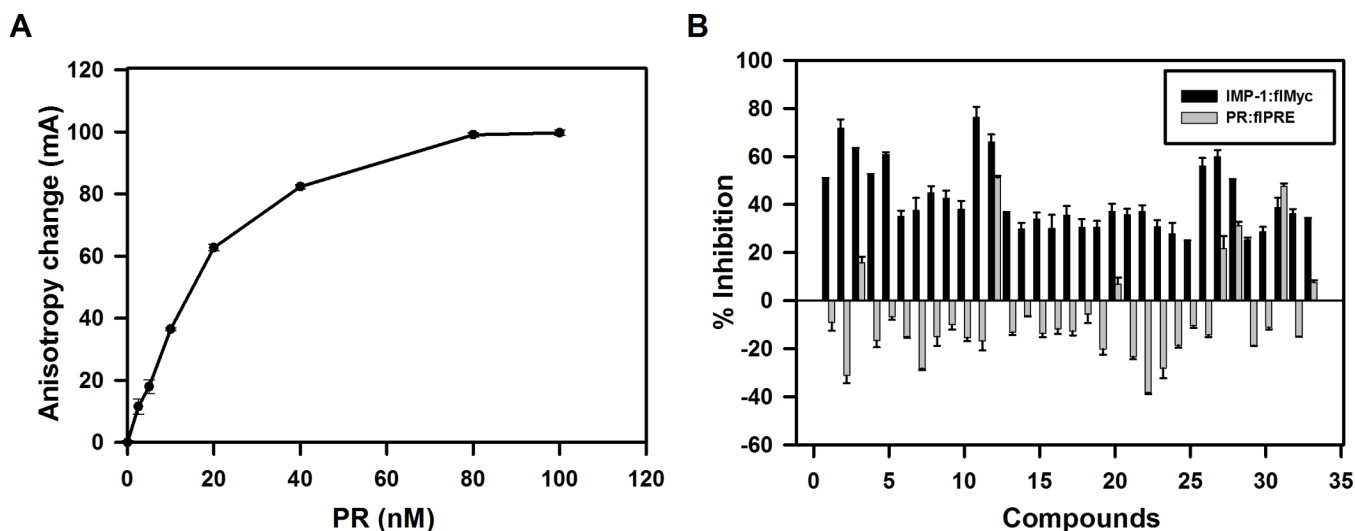


**Figure 4.**

Evaluation of hits for potency and specificity. Hits from the primary screen were verified and evaluated for specificity in follow-on assays. **(A)** Binding of purified PR-b to flPRE DNA probe. Increasing amounts of PR were incubated with 1 nM flPRE-DNA probe. Compounds were evaluated for specificity by testing compounds for inhibition of binding of PR to flPRE. **(B)** Primary hits were tested at 5 μM for the ability to inhibit binding of IMP-1 to flMyc RNA (black bars). Specificity of the verified hits was evaluated by testing their ability to inhibit binding of PR to flPRE at 10 μM (grey bars). Compounds that did not pass the verification assay were not assayed for inhibition of PR binding to flPRE and only data from all the verified hits is shown. Surprisingly, a substantial percentage of verified hits slightly increased binding of PR to the flPRE. The data in panel A and B represents the average ± SEM (n=4 (A); n=3 (B)).

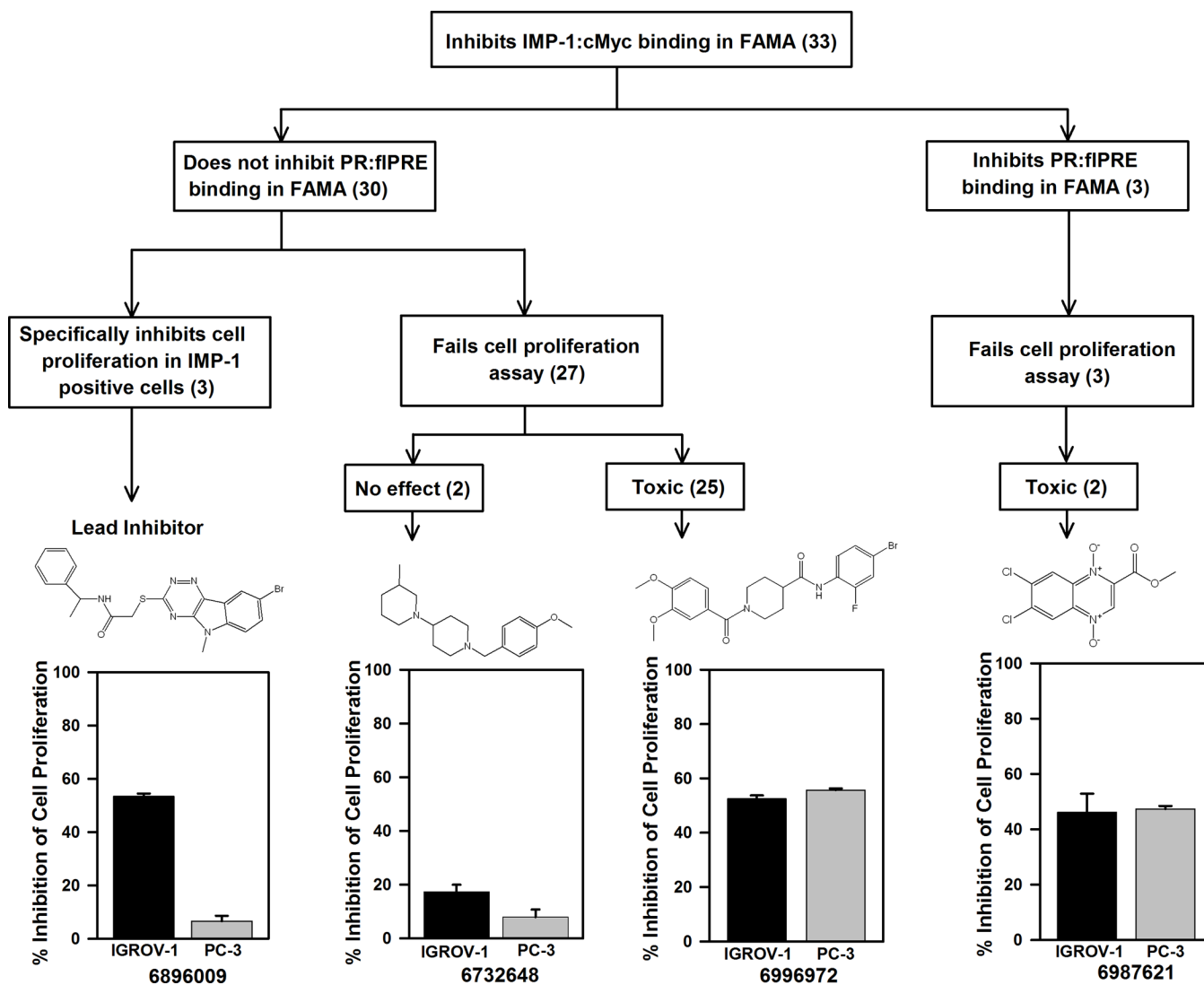


**Figure 5.**

Scheme for categorizing representative compounds from the pilot screen. Compounds were categorized based on their properties in FAMA and cell proliferation studies. Cell proliferation data for representative compounds in each category is presented below their structures and the Chembridge number is shown. Compounds were assayed at 20  $\mu$ M in IMP-1 positive IGROV-1 cells and in IMP-1 negative PC-3 cells. The 4 categories (from left to right) are the lead IMP-1 inhibitor; a compound that passed the IMP-1 inhibition and PR inhibition assays, but did not inhibit proliferation of either cell line; a compound that passed the IMP-1 and PR assays and exhibits non-specific toxicity because it inhibits proliferation of both the IGROV-1 cells and the IMP-1 negative PC-3 cells; and a compound that failed the specificity test because it inhibited PR binding to the PRE and also was toxic to the PC-3 cells. Set to 100% was cell proliferation for each cell line treated with DMSO vehicle. The data represents the average  $\pm$  SEM (n=4).

**Table 1**

## Summary of Statistical Data from the Pilot Screen

Number of compounds screened	17,600
Total hits	57
Overall hit rate (%)	0.30
Percentage repeat	58
Number of compounds repeated	33
Mean Z'-factor	0.60 ± 0.06

Details of the pilot screen are in the text. Experimental data from the pilot screen is in Figure 3 and Supplementary Figure 2.